Large orbital magnetic moment and its quenching in the itinerant uranium intermetallic compounds $UTGa_5$ (T=Ni, Pd, Pt)

K. Kaneko,[1,*] N. Metoki,[1,2] N. Bernhoeft,[3] G. H. Lander,[1,4] Y. Ishii,[1] S. Ikeda,[1] Y. Tokiwa,[1] Y. Haga,[1] and Y. Ōnuki[1,5]
[1]*Advanced Science Research Center, Japan Atomic Energy Research Institute, Tokai, Naka, Ibaraki 319-1195, Japan*
[2]*Department of Physics, Tohoku University, Sendai 980-8578, Japan*
[3]*DRFMC-CEA, 38054 Grenoble, France*
[4]*European Commission, JRC, Institute for Transuranium Elements, Postfach 2340, D-76125 Karlsruhe, Germany*
[5]*Graduate School of Science, Osaka University, Toyonaka, Osaka 560-0043, Japan*
(Received 14 July 2003; published 15 December 2003)

The crystal structure, lattice strain due to the antiferromagnetic ordering, and magnetic form factor in the itinerant $5f$ compounds $UTGa_5$ (T=Ni, Pd, Pt) have been studied by neutron scattering. High-resolution powder diffraction revealed that the tetragonality of the U-Ga layers increases down to the series of the transition metal element T. The integrated intensities of the antiferromagnetic reflections can be well explained with the Néel-type structure for $UNiGa_5$, whereas $UPtGa_5$ has the antiferromagnetic stacking of the ferromagnetically ordered uranium moments in the c plane. In both compounds the uranium moments orient along the c axis with moments of 0.75(5) and 0.32(5) μ_B for $UNiGa_5$ and $UPtGa_5$, respectively. No magnetic peak could be observed in the powder diffraction pattern of $UPdGa_5$ due to the small magnetic moment less than the experimental sensitivity. The orbital contributions in the magnetic form factor are reduced from the free-ion value, especially for $UNiGa_5$. This suppression shows a strong correlation with the bulk susceptibility. We observed lattice anomalies associated with the antiferromagnetic ordering. The tetragonality of the U-Ga layers is a sensitive measure of the nearest-neighbor interaction, the lattice anomaly and the orbital contribution suggest that orbital degrees of freedom may play an important role for the magnetic properties in these itinerant $5f$ antiferromagnets.

DOI: 10.1103/PhysRevB.68.214419 PACS number(s): 75.50.Ee, 61.12.Ex, 75.30.Kz, 75.90.+w

I. INTRODUCTION

Compounds incorporating f-electron elements have attracted much attention on account of their unusual magnetic and electronic properties, such as unconventional superconductivity and its coexistence with magnetic, ordering.[1] Examples include $4f$ rare earth electron systems based on Ce (Refs. 2–10) and Pr (Refs. 11,12), and $5f$ actinide compounds of U (Refs. 13–18) and Pu.[19,20]

Despite the considerable amount of work, there is still neither a consensus on a general mechanism nor an understanding as to why some compounds exhibit novel forms of superconductivity and others do not. Some empirical trends have however emerged: For instance, heavy fermion superconductivity is often realized in the vicinity of a quantum critical point (QCP) to a magnetic state induced, for example, by suppression of the magnetic critical temperature by alloying or hydrostatic pressure. A second recurrent theme is the presence of a similar crystal structure. A first set of compounds which exhibit possible unconventional superconducting pairing mechanisms comprises rare earth or uranium elements incorporated in a body-centered tetragonal lattice as seen in the compounds: $CeCu_2Si_2$,[2] $CeCu_2Ge_2$,[3] $CePd_2Si_2$,[4] $CeRh_2Si_2$,[5,6] and URu_2Si_2.[14] Another family, with apparent d-wave superconductivity, is $CeTIn_5$,[8–10] which has a crystal structure consisting of the sequential stacking of a transition metal (T) and $CeIn_3$ layer. Pure $CeIn_3$ also exhibits superconductivity, but only under pressure in the vicinity of a magnetic QCP.[7] Such stacked structures have been considered to enhance the nominal degree of two dimensionality in the electronic structure, which may play an important role in the formation of the emerging superconducting state.[21]

In this context, it is interesting that the recently discovered actinide high-T_C heavy fermion superconductors, $PuCoGa_5$ (Ref. 19) and $PuRhGa_5$,[20] are isostructural with $CeTIn_5$. Prior to the Pu systems, $UTGa_5$ compounds were studied;[22–25] however, despite the recent availability of high quality single crystalline samples, no superconductivity has been reported either at ambient or under high pressure.[26–31] Likewise, to date, there has been no report concerning the superconductivity in the Np-115 family.[20] One suggestion for the absence of superconductivity in $UTGa_5$ might be the strong hybridization and itinerant character of $5f$ levels, which leads to a relatively wide $5f$ band at E_F and a lack of spin fluctuations.[32–34] $UTGa_5$ compounds for T=Fe, Ru, Os, Co, Rh, and Ir show Pauli-paramagnetic behavior which suggests an itinerant character of the polarized electronic levels, while $UTGa_5$ compounds with T=Ni, Pd, and Pt exhibit itinerant antiferromagnetic ordering below their respective Néel temperatures T_N=86 K,[26] 30 K,[25] and 26 K.[28] In the case of the Pauli-paramagnetic compounds, $UFeGa_5$, $UCoGa_5$, and $URhGa_5$, the Fermi surfaces have been systematically studied and reveal a two-dimensional topology. The observed extremal areas are well explained in terms of calculations incorporating $5f$ electron levels in the conduction band.[35] Recent advances in band theory have also succeeded in reproducing experimentally compatible Fermi surface topologies in the antiferromagnetic compounds $UNiGa_5$ and $UPtGa_5$, which carry a sizeable magnetic moment.[36–38] These calculations reveal the d bands, prima-

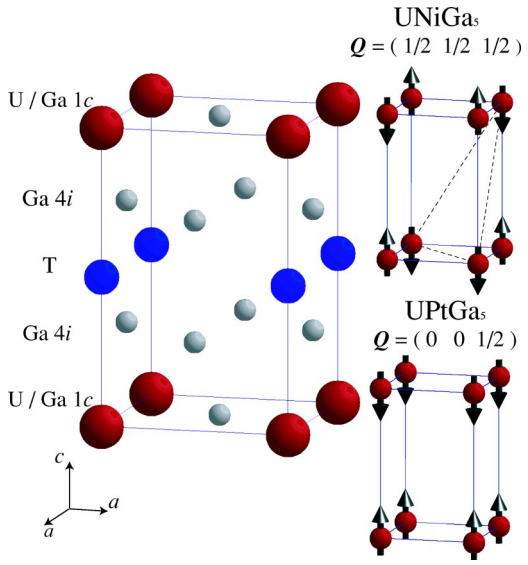

FIG. 1. (Color online) Crystal and antiferromagnetic structure of $UTGa_5$.[39]

rily associated with the transition metal element *T*, to be fully occupied whereas the hybridized U($5f$)-Ga($4p$) level supports the conduction band.[35,36,38] This explains the negligible moment on transition-metal element site and justifies more qualitative rigid-band models, which assume the full occupancy of the transition metal *d* band. The calculations suggest that the U($5f$)-Ga($4p$) hybridized conduction band has a high density of states at the Fermi level in the paramagnetic phase. This may be viewed as the origin of the (itinerant) antiferromagnetic instability in these compounds.

Such calculations, predicting filled *d* states on progressing through the $3d$ to $5d$ transition-metal series, suggest the electronic structure and the Fermi surface (at least in the paramagnetic state) should be almost identical. However, neutron-diffraction studies reveal the magnetic structures of $UNiGa_5$ and $UPtGa_5$ to be different, see Fig. 1.[39] The magnetic configuration of $UNiGa_5$ is based on two interpenetrating sublattices in a classic Néel-type ordering. The adjacent uranium moments are aligned in opposite directions, in a structure similar to the *G*-type antiferromagnetic configuration adopted by the simple cubic uranium lattice of UGa_3.[40–42] On the other hand, $UPtGa_5$ has an antiferromagnetic stacking along the tetragonal *c* axis of ferromagnetically ordered uranium moments in the basal plane. The difference in the two magnetic structures is significant since it implies a sign change of the nearest-neighbor interaction.

It thus remains an open question as to why, on cooling below T_N, the magnetic structures should be so different. One suggestion is that the lattice expansion caused by the increasing ionic radius of the transition-metal element may control the sign of the magnetic interaction between adjacent uranium ions when orbital degrees-of-freedom play an important role.[39]

To address this issue we report on (i) the crystal structure including the positional parameter for Ga $4i$ site z_{Ga}, (ii) the thermal evolution of the chemical unit-cell dimension and z_{Ga} below and above T_N, and (iii) the magnetic form factor to assess the orbital contribution. In this manner, we hope to cast fresh light on the role of effective chemical strain on the UGa_3 units, i.e., change in geometry relative to that of pure UGa_3, and the contribution of the orbital to the magnetic degrees-of-freedom, respectively.

II. EXPERIMENT

The polycrystalline samples for T=Ni, Pd, and Pt were synthesized by arc-melting stoichiometric amounts of the materials under argon gas atmosphere and subsequent annealing in an evacuated quartz tube at 650 °C for 90 h. We observed a single phase in $UNiGa_5$ and $UPtGa_5$, while small amounts of U_2PdGa_8 were detected in $UPdGa_5$. On the other hand, the single-crystal samples of $UNiGa_5$ and $UPtGa_5$ were grown by Ga self-flux method, with a typical sample size of $2.0\times3.6\times1.0\,mm^3$. A suitable single crystal of $UPdGa_5$ was not available for neutron scattering experiments. The details for the sample preparation technique have been published elsewhere.[26,28,29]

Two sets of neutron scattering experiments were carried out at the research reactor JRR-3 of the Japanese Atomic Energy Research Institute, Tokai, Japan.

First, neutron powder diffraction data were collected on the high-resolution powder diffractometer (HRPD) to determine the structural parameters at incident energy $E_i = 24.6\,meV$, $\lambda = 1.823$ Å with angular resolution of about 0.1 °, using a Ge (5 3 3) monochromator and collimation of 12′-12′-6′. The powder diffraction patterns thus obtained were analyzed by the Rietveld refinement method using RIETAN-2000 software.[43] Stoichiometric full site occupancy was assumed; we found that any defects are negligible in our present polycrystalline samples.

Second, the magnetic form factor was measured on single crystals of $UNiGa_5$ and $UPtGa_5$ using thermal neutron triple-axis spectrometers TAS-1 and TAS-2 collecting data in the (h 0 l) and (h h l) scattering planes. Pyrolytic graphite (PG) monochromator and analyzer crystals were employed with a ^{3}He detector at E_i=33 meV or 40 meV together with PG filters having a total thickness of 8 cm to reduce the contamination of higher-order Bragg harmonics. All collimation, except that in front of the monochromator, was removed and the background scattering from the sample cell and the cryostat was eliminated by a pair of beam slits giving a combined sample-spectrometer mosaic spread of $\omega \approx 0.3°$. The signal intensity was obtained by integration over θ-2θ and/or ω scans. The relative intensities of the integrated nuclear peaks measured in this manner are compared well with structure factor calculations based on the HRPD measurements and this served as a cross check on both the single-crystal stoichiometry and the general measurement technique. Note that the data are not biased by appreciable extinction effects. The magnetic contribution was extracted by subtracting the harmonic contaminations, measured at $T > T_N$, where T_N is the Néel temperature, and put on an absolute scale by calibration against selected nuclear peaks. The powder-diffraction data were unavailable for the form-factor analysis due to the small magnetic moment.

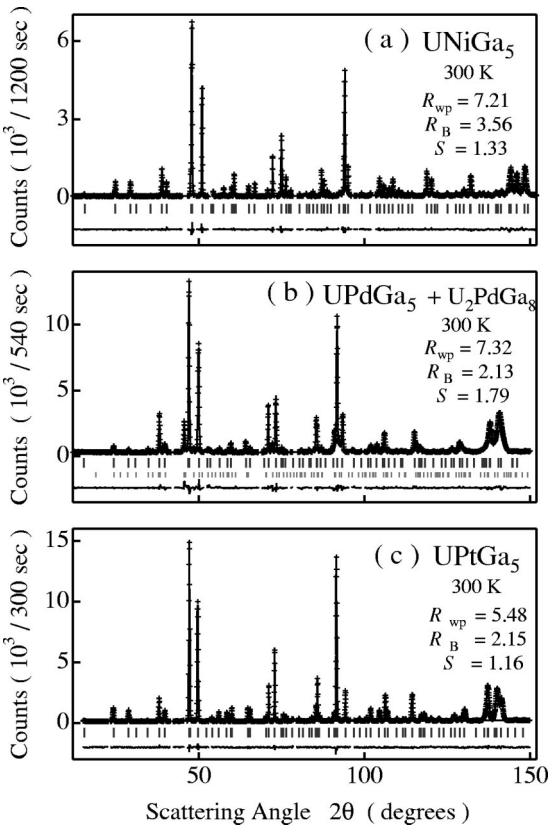

FIG. 2. Neutron powder diffraction pattern of (a) $UNiGa_5$, (b) $UPdGa_5$, and (c) $UPtGa_5$, respectively. The crosses are the measured data. The solid lines are calculated results after Rietveld refinement, based on the $HoCoGa_5$ structure. The positions of the peaks are denoted by small bars. The deviation of the calculation from experimental data, $I_{obs}-I_{cal}$, is also plotted at the bottom of each panel. A small portion of U_2PdGa_8 was detected as an impurity phase of $UPdGa_5$.

III. RESULTS

A. Crystal structure

Figure 2 shows representative powder-diffraction data of $UTGa_5$ measured at 300 K for T=Ni, Pd, and Pt in Figs. 2(a), 2(b), and 2(c), respectively. Structural and statistical significance, or reliability, parameters are summarized in Table I for typical measured temperatures. The quality of data is significantly better than that in our previous study due to improvements both in experimental and analysis techniques.[39] The HRPD data confirm a tetragonal $HoCoGa_5$ structure, which, to aid discussion, it is convenient to represent as sheets of UGa_3 blocks in a basal plane stacked along the tetragonal, c axis, with intercalating sheets of transition metal ions, Fig. 3. In this structure there are pure Ga($4i$) basal layers, which lie interstitial between the mixed U-Ga($1c$) and pure T basal layers. The relative in-cell location of the pure Ga($4i$) basal layers is given by the positional parameter z_{Ga}. This parameter is then used to define a degree of interlayer tetragonality between the U-Ga($1c$) and pure Ga($4i$) planes, i.e., the local distortion of the UGa_3 unit from that in the cubic UGa_3 compound. Thus the local tetragonality t is generalized from $t=1-(c/a)$ to:

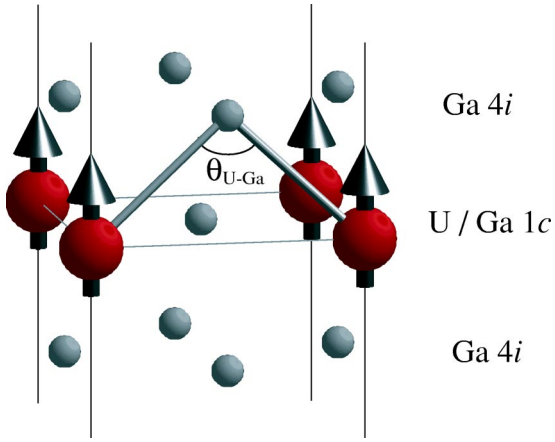

FIG. 3. (Color online) The tetragonality between the Ga($4i$) and U-Ga($1c$) layers in $UTGa_5$. The interplaner U-Ga($4i$)-U bond angle $\theta_{U\text{-}Ga}$ corresponds to $\theta_{U\text{-}Ga}=\pi-2\arctan(2cz_{Ga}/a)$.

$$t=1-(2cz_{Ga}/a) \tag{1}$$

where, in Eq. (1), positive tetragonality indicates the U-Ga layer to be compressed along c axis compared with the cubic UGa_3 which has the $AuCu_3$ structure.

We find that in the $UTGa_5$ system there are systematic differences in the generalized tetragonality between the pure Ga($4i$) and U-Ga($1c$) layers together with the corresponding interplanar U-Ga($4i$)-U bond angle $\theta_{U\text{-}Ga}=\pi-2\arctan(2cz_{Ga}/a)$, see Fig. 3. The generalized tetragonality coefficient increases markedly from $t=1.5\%$ in $UNiGa_5$ to $t=7.0\%$ in $UPtGa_5$. Correspondingly, the bond angle $\theta_{U\text{-}Ga}=90.9°$ in $UNiGa_5$ is very close to 90° expected in a local cubic symmetry while in contrast, both $UPdGa_5$ with $t=5.4\%$ and $\theta_{U\text{-}Ga}=93.0°$ and $UPtGa_5$ at $\theta_{U\text{-}Ga}=94.2°$ deviate significantly.

As suggested, it is instructive to consider the unit cell as a superposition of UGa_3 units in the basal plane separated by a T metal layer. It is then apparent that the basal plane UGa_3 units in $UNiGa_5$ are very close to pure UGa_3 both in U-Ga-U bond angle (i.e., local cubic symmetry) and basal plane lattice parameter $a=4.238$ Å ($UNiGa_5$) and 4.248 Å (UGa_3) at 300 K.[44] The increases in a and the decrease in z_{Ga} down the series of $UTGa_5$ (T=Ni, Pd, Pt), without a proportional increase in c, act to distort the UGa_3 block as if under uniaxial compression increasing the U-Ga-U bond angle giving a new magnetic structure with a concurrent reduction of T_N.

We can furthermore calculate the distance from a U atom to the two Ga atoms, one in the basal tetragonal plane [Ga($1c$)] and the other in the next plane (see Figs. 1 and 3) at z along the c axis Ga($4i$). The U-Ga($1c$) distance steadily increases down to the series from 2.98 Å in $UNiGa_5$ to 3.06 Å in $UPtGa_5$, whereas the U-Ga($4i$) distance averages 2.962 with a standard deviation of ±0.004 Å for all three materials. (All using the low-temperature lattice parameters.) The difference between U-Ga($1c$) and Ga($4i$) thus increases from the insignificant 0.03 Å in the Ni compound to 0.10 Å

TABLE I. Structural parameters a, c, z_{Ga} of $UTGa_5$ (T=Ni, Pd, Pt) determined from the Rietveld analysis of neutron powder-diffraction data at selected temperatures. Uranium atoms are located at $1a$ (0, 0, 0), T at $1b$ $(0,0,\frac{1}{2})$, Ga at $1c(\frac{1}{2},\frac{1}{2},0)$, and $4i(0,\frac{1}{2},z_{Ga})$, where z_{Ga} is a positional parameter. The tetragonality of U-Ga layer t obtained by Eq. (1) and the bond angle $\theta_{U\text{-}Ga}$ are also listed. R_{wp}, S, and R_B are conventional reliability factors.[43]

	T (K)	a (Å)	c (Å)	z_{Ga}	t (%)	$\theta_{U\text{-}Ga}$	R_{wp}	S	R_B
$UNiGa_5$	9.0	4.2246(1)	6.7751(1)	0.3070(1)	1.51	90.87(1)	8.31	1.62	4.11
(T_N=86 K)	86.7	4.2272(1)	6.7708(1)	0.3070(1)	1.70	90.98(1)	7.32	1.45	3.45
c/a=1.604	300	4.2380(1)	6.7864(1)	0.3074(1)	1.55	90.89(1)	9.65	1.33	3.56
$UPdGa_5$	3.0	4.3101(1)	6.8428(1)	0.2980(1)	5.37	93.16(1)	9.87	1.82	5.3
(T_N=30 K)	29.7	4.3099(1)	6.8435(1)	0.2979(1)	5.40	93.18(1)	9.50	1.76	4.91
c/a=1.587	300	4.3218(1)	6.8637(1)	0.2987(1)	5.12	93.01(1)	7.32	1.79	2.13
$UPtGa_5$	7.5	4.3281(1)	6.7889(1)	0.2965(1)	6.97	94.14(1)	8.00	1.65	5.30
(T_N=26 K)	26.3	4.3275(1)	6.7880(1)	0.2964(1)	7.01	94.16(1)	7.16	1.48	5.40
c/a=1.568	300	4.3386(1)	6.8054(1)	0.2964(1)	7.02	94.17(1)	5.61	1.16	2.15

in the Pt compound. It is this change with the heavier T substitutions, and the resulting change in the hybridization and exchange interactions, that probably gives rise to the different magnetic structure.

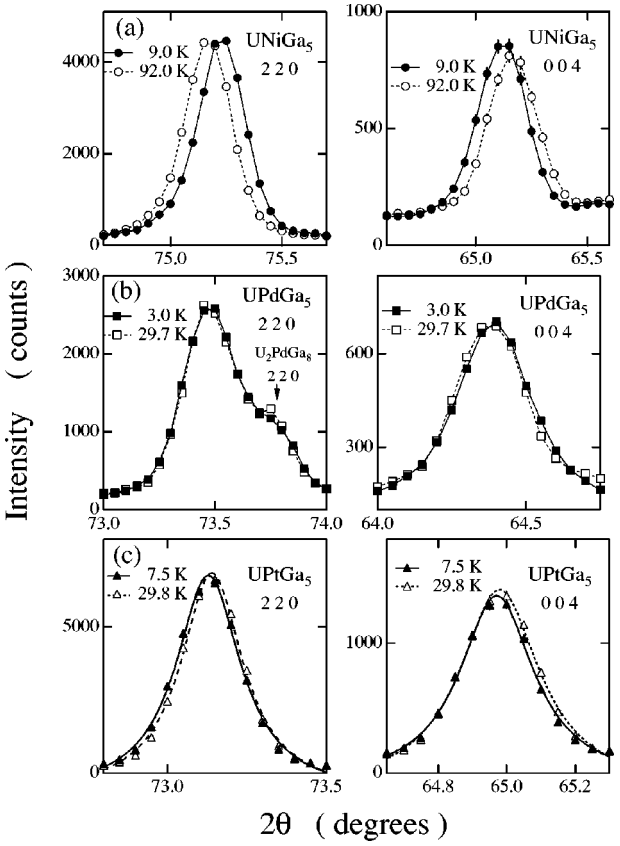

FIG. 4. The neutron powder-diffraction profiles of the basal plane 2 2 0 and out-of-plane 0 0 4 reflections. The data, measured below and above T_N, are denoted by solid and open symbols, respectively. The solid ($T<T_N$) and dotted ($T>T_N$) lines are the fitting results after Rietveld refinement. The panels (a), (b), and (c) indicate the data for $UNiGa_5$, $UPdGa_5$, and $UPtGa_5$, respectively.

B. Temperature dependence of structural parameters

The high-angle powder-diffraction patterns around the 2 2 0 and 0 0 4 reflections are shown in Fig. 4 for $UTGa_5$ (T=Ni, Pd, Pt). With decreasing temperature below T_N, the 2 2 0 and 0 0 4 reflections of $UNiGa_5$ shift to the higher and lower scattering angle, respectively, implying the lattice constant a of $UNiGa_5$ to decrease while c increases in the antiferromagnetically ordered phase. In $UPdGa_5$, the thermal expansion in the a direction is almost canceled out by the magnetostrictive anomaly while the c direction exhibits a small shift. On the other hand, for $UPtGa_5$, both the 2 2 0 and 0 0 4 reflections shift slightly towards the lower scattering angle, indicative of a lattice expansion below T_N.

These qualitative observations have been quantified by a careful Rietveld refinement of the neutron powder-diffraction data. The lattice constants, which show an anomaly at T_N are given in Figs. 5(a)–(c) for $UNiGa_5$, $UPdGa_5$, and $UPtGa_5$, respectively. At base temperature, 9.0 K, $UNiGa_5$ exhibits a relative increase in a of about 0.1% and decrease in c about 0.04% compared with their respective values at T_N.

The lattice parameter a in $UPdGa_5$ exhibits a quasi-invar-like plateau below T_N, indicating a magnetoelastic interaction in the basal plane, which essentially compensates the paramagnetic thermal contraction, whereas the c axis exhibits a monotonous decrease with decreasing temperature.

The lattice constants in $UPtGa_5$ increase by $\sim$0.013 % at base temperature relative to their value at T_N in both a- and c-directions as shown in Fig. 5(c). Thus the lattice expansion due to the magnetic ordering is estimated as $\sim$0.02 % after subtracting the thermal contraction $\sim$0.07 % estimated by extrapolation from the paramagnetic state. The relatively more important values of thermal expansion in $UNiGa_5$ correlates with its elevated Néel temperature and magnetic moment. The lattice contraction of a in $UPtGa_5$ is opposite from the lattice expansion in $UNiGa_5$, while intermediate behavior is found in $UPdGa_5$.

The change in sign of the basal plane contribution to the thermal expansion between the two compounds $UNiGa_5$ and $UPtGa_5$ may reflect the different, antiferromagnetic as op-

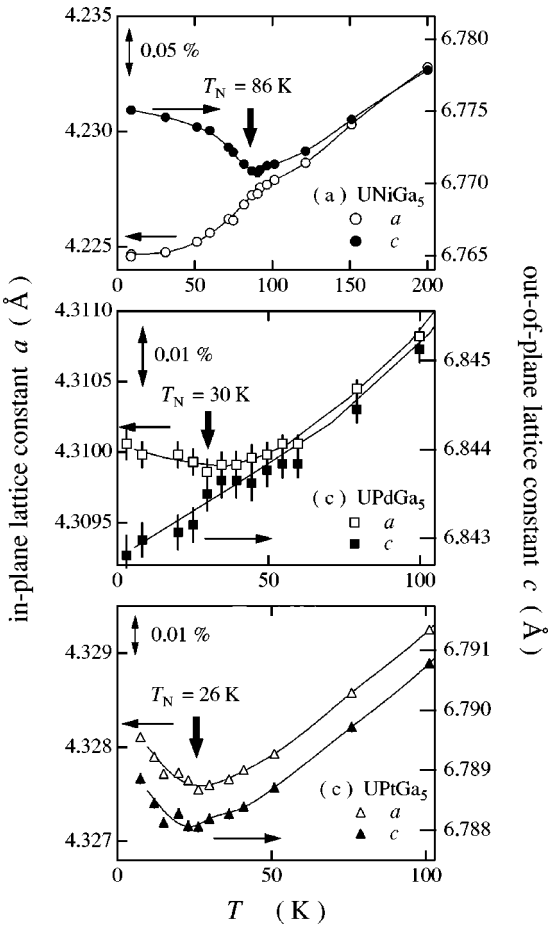

FIG. 5. Temperature dependence of the basal and out-of-plane lattice constants a and c denoted by open and close symbols, respectively, for (a) $UNiGa_5$, (b) $UPdGa_5$, and (c) $UPtGa_5$. The lines are a guide to the eyes.

posed to ferromagnetic, coupling in $UNiGa_5$ and $UPtGa_5$, respectively. This situation suggests the presence of a critical separation ε_0, where the effective U-U basal plane interaction changes sign:

$$H=\sum -I^{ij}_{(\varepsilon)}J^iJ^j, \tag{2}$$

$$I^{ij}<0 \ \text{(antiferromagnetic; } UNiGa_5\text{)} \ \text{for} \ \varepsilon<\varepsilon_0,$$

$$I^{ij}>0 \ \text{(ferromagnetic; } UPtGa_5\text{)} \ \text{for} \ \varepsilon>\varepsilon_0.$$

On the other hand, the antiferromagnetic coupling as well as the negative thermal expansion for c axis is common to $UNiGa_5$ and $UPtGa_5$.

The ab plane invarlike anomaly of $UPdGa_5$, together with the lack of spontaneous magnetization,[25] suggests the magnetic structure of this compound may be composed of ferromagnetic UGa_3 basal plane blocks antiferromagnetically stacked along c as in $UPtGa_5$. To date, however, no antiferromagnetic peak has been observed in neutron powder-diffraction experiments, possibly on account of a small ordered moment lying below our experimental sensitivity

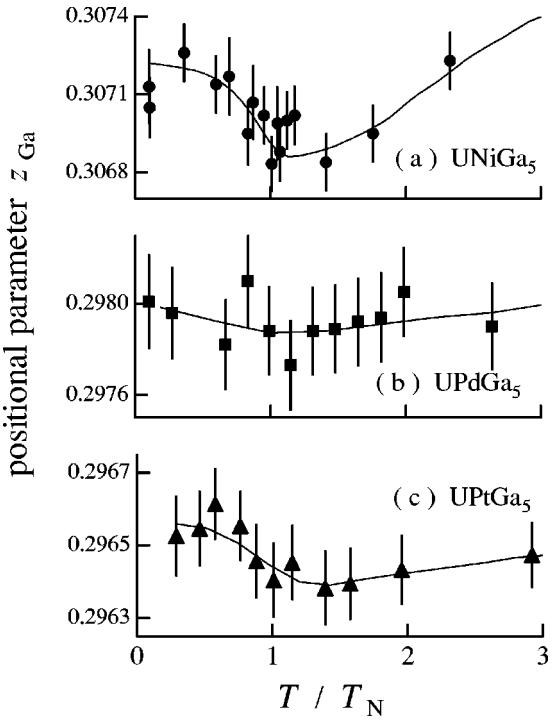

FIG. 6. Temperature dependence of the z parameter of Ga atoms at $4i$-site, z_{Ga}, for (a) $UNiGa_5$, (b) $UPdGa_5$, and (c) $UPtGa_5$, respectively.

$\sim 0.4\mu_B$/U. In order to clarify the magnetic structure, a single-crystal sample will be required.

Figure 6 summarizes the z parameter of the Ga-4i site, z_{Ga} as a function of temperature. The magnitude of the z_{Ga} parameter decreases down to the series of the transition element T=Ni, Pd, Pt and this, coupled with the increase of a, drives the U-Ga($4i$)-U bond distortion referred to above. However, while sensitive to the phase transition, this internal parameter does not respond in a dramatic fashion to the magnetostrictive anomaly having a maximal relative decrease of ~ 0.001.

C. Magnetic form factors

The magnetic form factor was obtained by measuring the intensity of antiferromagnetic reflections. The integrated intensity of magnetic Bragg peak is expressed as,

$$I_{\text{mag}}(\boldsymbol{Q})\propto|F_{mag}(\boldsymbol{Q})|^2\mu^2f^2(\boldsymbol{Q})(\sin\alpha)^2L(\theta), \tag{3}$$

where F_{mag} is the magnetic structure factor, $f(\boldsymbol{Q})$ is the magnetic form factor, α is the angle between the ordered magnetic moment and the scattering vector $\boldsymbol{Q}$, and $L(\theta)$ is the Lorentz factor. The magnetic structure factor F_{mag} is constant in both magnetic configurations of $UNiGa_5$ and $UPtGa_5$. The magnetic form factors were thus derived by normalizing the antiferromagnetic intensity with Lorentz and angular factors in Eq. (3).

Within the dipole approximation the magnetic form factor may be expressed by the sum of the spin and orbital contribution $f_S(Q)$ and $f_L(Q)$,[45]

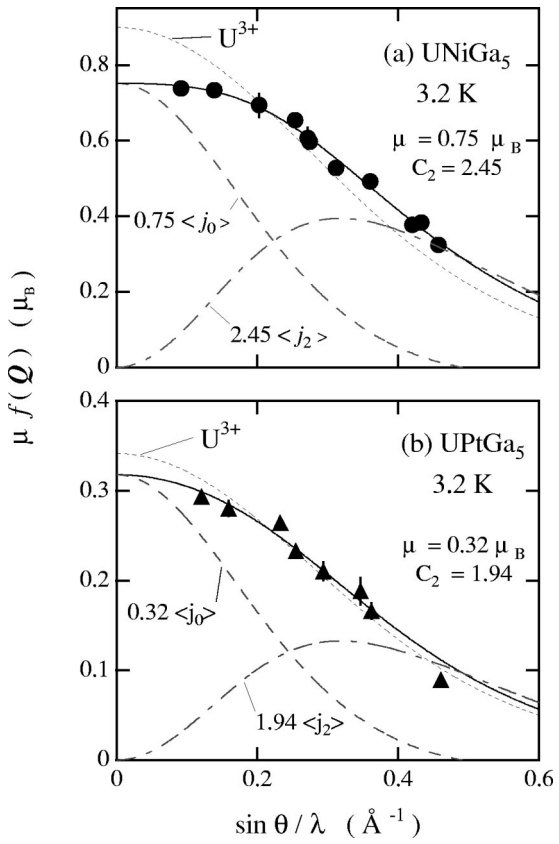

FIG. 7. The experimentally obtained magnetic form factors for (a) $UNiGa_5$ and (b) $UPtGa_5$ denoted by circles and triangles, respectively. The solid lines are the best fit of the calculated form factors using Eq. (7) with μ and C_2 as fitting parameters. The dotted line indicates the magnetic form factor for U^{3+} free ion. The dashed line and dash-dot line show the calculated curves for $\langle j_0 \rangle$ and $\langle j_2 \rangle$ terms, respectively.

$$\mu f(Q) = \mu_S f_S(Q) + \mu_L f_L(Q). \tag{4}$$

where μ_S and μ_L are the spin and orbital moment, respectively.

The individual form factors are then expanded in the basis of Bessel functions,

$$f_S(Q) \sim \langle j_0 \rangle \tag{5}$$

$$f_L(Q) \sim \langle j_0 \rangle + \langle j_2 \rangle. \tag{6}$$

Thus, with the total moment $\mu = \mu_S + \mu_L$, we get

$$\mu f(Q) = \mu(\langle j_0 \rangle + C_2 \langle j_2 \rangle), \tag{7}$$

$$\text{where } C_2 = \mu_L / \mu,$$

$$\mu_L / \mu_S = C_2 / (1 - C_2).$$

The experimental form factors, given in Fig. 7, have been decomposed using Eq. (7). The result of a least square fitting to the moment μ and C_2 coefficient is denoted by the solid curves and values of μ, μ_L, μ_S, and C_2 for $UNiGa_5$ and $UPtGa_5$ are listed in Table II.

TABLE II. Fitting results of total magnetic moment μ, orbital and spin magnetic moment μ_L and μ_S, $|\mu_L/\mu_S|$ and C_2 for U^{3+}, $UPtGa_5$, $UNiGa_5$, and UGa_3.[44]

	μ (μ_B)	μ_L (μ_B)	μ_S (μ_B)	$\lvert\mu_L/\mu_S\rvert$	C_2
U^{3+}				2.56	1.64
$UPtGa_5$	0.32(5)	0.62(7)	−0.30(7)	2.10(20)	1.94(17)
$UNiGa_5$	0.75(5)	1.84(7)	−1.09(7)	1.68(4)	2.45(7)
UGa_3[44]	0.63(5)	1.5(1)	−0.9(1)	1.66(5)	2.52(5)

The most remarkable thing is the large orbital contribution, which is characteristic to the uranium intermetallic compounds based on itinerant $5f$ electrons.[45] However, we found that the contribution of the orbital moments μ_L/μ_S is strongly suppressed in $UTGa_5$ from the value for U^{3+} free ion. For comparison the values of C_2 and μ_L/μ_S for U^{3+} with f^3 configuration are also described in Table II. $|\mu_L/\mu_S| = 1.68$ for $UNiGa_5$ is much smaller than the value of U^{3+} free ion, $|\mu_L/\mu_S| = 2.56$. $|\mu_L/\mu_S| = 2.10$ for $UPtGa_5$ is also smaller than that of U^{3+} free ion. The suppression of μ_L can be recognized in the large contribution of $\langle j_2 \rangle$ term denoted by dash-dot lines in Fig. 7. The dotted lines in Fig. 7 represent the magnetic form factor for U^{3+} free ion, which clearly deviates from the experimental data, especially for $UNiGa_5$.

A large orbital contribution and the suppression of the magnetic orbital moment has been reported in UGa_3.[44] The results for UGa_3 are summarized in Table II for comparison. The suppression of μ_L in UGa_3 was also confirmed with our own sample.[46] The C_2 as well as μ_L/μ_S in $UNiGa_5$ are very similar to those for UGa_3. We understand this to be related to the similarity of the structure in U-Ga layer and the resulting itinerancy of the $5f$ states.

IV. DISCUSSION

Figure 8 gives the bulk, $q=0$, magnetic susceptibility χ of UGa_3 and $UTGa_5$ (T=Ni, Pd, Pt) as a function of temperature.[26,47,28] It is seen that the paramagnetic low-temperature susceptibility is enhanced in the order Ni<Pd<Pt which correlates with the local tetragonality of the U-Ga layers.

$UNiGa_5$ has the similar bulk magnetic susceptibility to UGa_3 (Ref. 48) as well as the local structure. Above T_N, χ of $UNiGa_5$ lies below 2×10^{-3} emu/mol, is more or less isotropic and exhibits a weak temperature dependence. Below T_N, $\chi \| c$ decreases by a factor ~ 2 falling to the magnitude of the Pauli paramagnetic susceptibility in $UCoGa_5$.[49] The larger discontinuity in $\chi \| c$ than in $\chi \| a$ below T_N is consistent with the antiferromagnetic structure having the uranium moment parallel to the c axis.

The magnetic susceptibility of $UPdGa_5$ in the paramagnetic regime has a small anisotropy and a temperature dependence that is hard to reconcile with a Curie-Weiss behavior. Further investigations of this composition, behaving as it does in an intermediate fashion between the itinerant Ni intercalated and more strongly localized behavior of the Pt intercalated materials, will be most interesting as single crys-

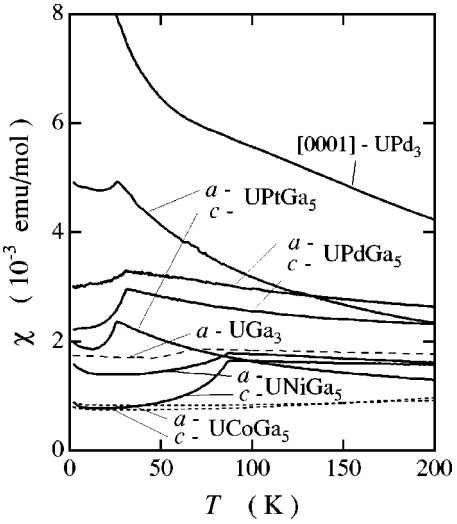

FIG. 8. Magnetic susceptibility of $UNiGa_5$, $UPdGa_5$, and $UPtGa_5$. The broken line and dotted lines are the magnetic susceptibilities for UGa_3 (Ref. 48) and $UCoGa_5$.[49] The magnetic susceptibility along the [0001] direction in UPd_3 is also displayed as a typical example for the $5f$ localized system.[50]

tals become available for both x-ray and neutron scattering techniques.

In $UPtGa_5$ the magnetic susceptibility has a much stronger anisotropy and temperature dependence. Again, in agreement with our neutron diffraction data, this is suggestive of a more localized character of the uranium moment with the increasing transition-metal ion radius and concomitant distortion of the local UGa_3 symmetry. The effective paramagnetic moments are, however, still rather small $1.1\mu_B$ ($\boldsymbol{H}\|a$) and $1.85\mu_B$ ($\boldsymbol{H}\|c$) compared with those for U^{3+} and U^{4+} free ion of 3.62 μ_B and 3.58 μ_B, respectively.

Tables I and II indicate the orbital contribution to correlate with the local U-Ga structure and the magnetic susceptibility. Orbital polarization in itinerant magnets is possible, but few examples are known. In the present series of $UTGa_5$ compounds, the neutron diffraction data suggest a significant orbital contribution. To investigate the systematics, since the ordering temperatures and moments vary, it is useful to compare the ratios of orbital and spin to total moment across the series UGa_3, $UNiGa_5$ to $UPtGa_5$. Inspection of Table II shows that for UGa_3 and $UNiGa_5$ the scaled orbital and spin contributions to the net moment are closely similar. The almost comparable local U-Ga structure between UGa_3 and $UNiGa_5$ implies its definitive role on the orbital polarization as well as on the magnetic susceptibility mentioned above. In case of $UPtGa_5$, where the local distortion from cubic UGa_3 units is maximal, the ratio of spin and orbital moments, $|\mu_L/\mu_S|$, approaches more closely to that of the free U^{3+} ion, see Table II. The form-factor observations and the magnetic susceptibility suggest that the system may be regarded as more closely ionic with respect to the extent and symmetry of the uranium moment. However, while our result does not enforce a lack of itinerancy to the $5f$ levels, it may imply a reduced degree of U-Ga hybridiszation.

One of the more intriguing aspects is the relation between the local distortion and the magnetic structure; namely, the sign of the nearest-neighbor interaction is different between $UNiGa_5$ and $UPtGa_5$, see Fig. 1. This is a rather surprising result; $UNiGa_5$ and $UPtGa_5$ have an identical electronic structure and Fermi surface topology in the paramagnetic state, hence one expects the same magnetic structure. This anomalous behavior becomes clear on comparison with other systems, such as UT_2Si_2 ($T=3d$, $4d$, and $5d$ transition metal elements).[51,52] The nearest-neighbor interaction in the c plane in antiferromagnetic UT_2Si_2 is always ferromagnetic, despite the variety of materials.[53,54]

We have argued that the Ni compound is the closest, both structurally [smallest value of t in Table I and almost similar spacings U-Ga($1c$) and U-Ga($4i$)] and electronically (i.e., paramagnetic susceptibility, value of total moment, and $|\mu_L/\mu_S|$) to the pure UGa_3 material and, therefore, it is perhaps not surprising that the magnetic configurations of the two resemble each other, with nearest neighbor U atoms antiferromagnetically aligned. On the other hand, the increasing ''distortion'' of the U environment (see Fig. 3) as seen by the larger t values in Table I, appears to favor a planar configuration of the U moments, such that they form ferromagnetic planes stacked antiferromagnetically. The precise microscopic mechanism responsible for this change remains unclear, and it remains to be seen what the magnetic structures are of $UPdGa_5$ as well as the Np analog, $NpCoGa_5$.[20]

One possibility is that a concurrent orbital ordering, which would introduce a anisotropy and the difference in hybridization, takes place in $UTGa_5$, which affects on the change of basal plane magnetic configuration from antiferro to ferromagnetic order. The present study clarifies the relevant lattice distortion which corresponds to the different magnetic structure between $UNiGa_5$ and $UPtGa_5$. In this light it is noteworthy that recent NMR (Ref. 55) and resonant x-ray scattering[56] work on UGa_3 also suggest strong $5f$-$4p$ hybridization and the possibility of some form of orbital ordering. The enormous enhancement, $\sim$ 1000 fold, seen in pure UGa_3 in resonant x-ray scattering tuned to the Ga-$4p$ edge might be related to the degree of Ga hybridization with uranium $5f$ levels, this hypothesis may be tested by experiments on the $UTGa_5$ series. This systematic study expected to bring an origin of the enhancement into relief from diversified viewpoint: the different magnetic structure, hybridization and so on.

The comparable local chemical structure of pure UGa_3 and the UGa_3 basal plane blocks in $UNiGa_5$, reinforces the idea that one may regard the transition-metal intercalation in $UNiGa_5$ as serving primarily to define a unique symmetry axis on an otherwise undistorted UGa_3 system. The chemical unit-cell symmetry breaking obliges the moments to point along the tetragonal axis in a simple fashion unlike the case of UGa_3 where, despite intense efforts,[55,46] the moment direction is still unresolved. The spin and orbital polarization is some 20% stronger in the tetragonal symmetry, accompanying the change in Fermi surface topology towards two dimensionality.

In contrast in the $CeTIn_5$[8–10] series, which has a similar crystal packing consisting of a sequential stacking of a transition metal (T) and $CeIn_3$ layers, the trend is to become less

magnetic and have a developing superconductivity with increasing two dimensionality of the Fermi surface. Careful structural and form factor measurements in the $CeTIn_5$ series may be eminently worthwhile.

In conclusion, the weak temperature dependence, as well as the small magnitude of the bulk susceptibility, taken together with the partial quenching of the orbital moment in these materials, point to the itinerant nature of the $5f$ levels. Careful structural studies, combined with band-structure calculations, which indicate the transition metal *d* band to be full, suggest the primary role of the transition-metal intercalation is to change the equilibrium lattice parameter and thus affect the overlap of orbitals involved in $5f$-$4p$ bonding. It appears that the local distortion of the UGa_3 basal plane units, or equivalently the $5f$-$4p$ bonding, plays a major role in the stabilization of the different magnetic structures supported across the investigated series of compounds.

ACKNOWLEDGMENTS

Authors would like to thank H. Yamagami, T. Hotta, T. Maehira, H. Kato, S. Kambe, R. Walstedt, and H. Yasuoka for the stimulating discussions. Part of this work was financially supported by grant-in-Aid for Scientific Research from the Japanese Ministry of Education, Culture, Sport, and Technology.

*Electronic address: kanekok@neutrons.tokai.jaeri.go.jp

[1] For example, V. Sechovský and L. Havela, *Handbook of Magnetic Materials*, edited by K. H. J. Bushow (Elsevier, Amsterdam, 1998), Vol. 11, p. 1.

[2] F. Steglich, J. Aarts, C.D. Bredl, W. Lieke, D. Meschede, W. Franz, and H. Schäfer, Phys. Rev. Lett. **43**, 1892 (1979).

[3] F.R. de Boer, J.C.P. Klaasse, P.A. Veenhuizen, A. Böhm, C.D. Bredl, U. Gottwick, H.M. Mayer, L. Pawlak, U. Rauchschwalbe, H. Spille, and F. Steglich, J. Magn. Magn. Mater. **63&64**, 91 (1987).

[4] F.M. Grosche, S.R. Julian, N.D. Mathur, and G.G. Lonzarich, Physica B **223&224**, 50 (1996).

[5] R. Movshovich, T. Graf, D. Mandrus, J.D. Thompson, J.L. Smith, and Z. Fisk, Phys. Rev. B **53**, 8241 (1996).

[6] S. Araki, M. Nakashima, R. Settai, T.C. Kobayashi, and Y. Ōnuki, J. Phys.: Condens. Matter **14**, L377 (2002).

[7] N.D. Mathur, F.M. Grosche, S.R. Julian, I.R. Walker, D.M. Freye, R.K. W Haselwimmer, and G.G. Lonzarich, Nature (London) **394**, 39 (1998).

[8] R. Movshovich, M. Jaime, J.D. Thompson, C. Petrovic, Z. Fisk, P.G. Pagliuso, and J.L. Sarrao, Phys. Rev. Lett. **86**, 5152 (2001).

[9] H. Hegger, C. Petrovic, E.G. Moshopoulou, M.F. Hundley, J.L. Sarrao, Z. Fisk, and J.D. Thompson, Phys. Rev. Lett. **84**, 4986 (2000).

[10] C. Petrovic, R. Movshovich, M. Jaime, P.G. Pagliuso, M.F. Hundley, J.L. Sarrao, Z. Fisk, and J.D. Thompson, Europhys. Lett. **53**, 354 (2001).

[11] M.B. Maple, P.-C. Ho, V.S. Zapf, N.A. Frederick, E.D. Bauer, W.M. Yuhasz, F.M. Woodward, and J.W. Lynn, J. Phys. Soc. Jpn. **71**, Suppl., 23 (2002).

[12] E.D. Bauer, N.A. Frederick, P.-C. Ho, V.S. Zapf, and M.B. Maple, Phys. Rev. B **65**, 100506(R) (2002).

[13] G.R. Stewart, Z. Fisk, J.O. Willis, and J.L. Smith, Phys. Rev. Lett. **52**, 679 (1984).

[14] T.T.M. Palstra, A.A. Menovsky, J. van den Berg, A.J. Dirkmaat, P.H. Kes, G.J. Nieuwenhuys, and J.A. Mydosh, Phys. Rev. Lett. **55**, 2727 (1985).

[15] C. Geibel, C. Schank, S. Thies, H. Kitazawa, C.D. Bredl, A. Böhm, M. Rau, A. Grauel, R. Caspary, R. Helflich, U. Ahlheim, G. Weber, and F. Steglich, Z. Phys. B **84**, 1 (1991).

[16] H.R. Ott, H. Rudigier, Z. Fisk, and J.L. Smith, Phys. Rev. Lett. **50**, 1595 (1983).

[17] S.S. Saxena, P. Agarwal, K. Ahilan, F.M. Grosche, R.K.W. Haselwimmer, M.J. Steiner, E. Pugh, I.R. Walker, S.R. Julian, P. Monthoux, G.G. Lonzarich, A. Huxley, I. Sheikin, D. Braithwaite, and J. Flouquet, Nature (London) **406**, 587 (2000).

[18] D. Aoki, A. Huxley, E. Ressouche, D. Braithwaite, J. Flouquet, J.P. Brison, E. Lhotel, and C. Paulsen, Nature (London) **413**, 613 (2001).

[19] J.L. Sarrao, L.A. Morales, J.D. Thompson, B.L. Scott, G.R. Stewart, F. Wastin, J. Rebizant, P. Boulet, E. Colineau, and G.H. Lander, Nature (London) **420**, 297 (2002).

[20] F. Wastin, P. Boulet, J. Rebizant, E. Colineau, and G.H. Lander, J. Phys.: Condens. Matter **15**, S2279 (2003).

[21] P. Monthoux and G.G. Lonzarich, Phys. Rev. B **59**, 14598 (1999).

[22] Yu.N. Grin, P. Rogl, and K. Hiebl, J. Less-Common Met. **121**, 497 (1986).

[23] S. Noguchi and K. Okuda, J. Magn. Magn. Mater. **104-107**, 57 (1992).

[24] K. Okuda and S. Noguchi, in *Physical Properties of Actinide and Rare Earth Compounds*, edited by T. Kasuya, T. Ishii, T. Komatsubara, O. Sakai, N. Môri, and T. Saso, JJAP Series 8 (Publication Office, JJAP, Tokyo, 1993), p. 32.

[25] V. Sechovský, L. Havela, G. Schaudy, G. Hilsher, N. Pillmayr, P. Rogl, and P. Fischer, J. Magn. Magn. Mater. **104-107**, 11 (1992).

[26] Y. Tokiwa, Y. Haga, E. Yamamoto, D. Aoki, N. Watanabe, R. Settai, T. Inoue, K. Kindo, H. Harima, and Y. Onuki, J. Phys. Soc. Jpn. **70**, 1744 (2001).

[27] Y. Tokiwa, T. Maehira, S. Ikeda, Y. Haga, E. Yamamoto, A. Nakamura, Y. Onuki, M. Higuchi, and A. Hasegawa, J. Phys. Soc. Jpn. **70**, 2982 (2001).

[28] Y. Tokiwa, S. Ikeda, Y. Haga, T. Okubo, T. Iizuka, K. Sugiyama, A. Nakamura, and Y. Onuki, J. Phys. Soc. Jpn. **71**, 845 (2002).

[29] S. Ikeda, Y. Tokiwa, Y. Haga, E. Yamamoto, T. Okubo, M. Yamada, N. Nakamura, K. Sugiyama, K. Kindo, Y. Inada, H. Yamagami, and Y. Onuki, J. Phys. Soc. Jpn. **72**, 576 (2003).

[30] M. Nakashima, Y. Tokiwa, H. Nakawaki, Y. Haga, Y. Uwatoko, R. Settai, and Y. Onuki, J. Nucl. Sci. Technol., Suppl. **3**, 214 (2002).

[31] M. Nakashima, Y. Haga, E. Yamamoto, Y. Tokiwa, M. Hedo, Y. Uwatoko, R. Settai, and Y. Onuki, J. Phys.: Condens. Matter **15**, S2007 (2003).

[32] J. D. Thompon (private communications).

[33] I. Opahle and P.M. Oppeneer, Phys. Rev. Lett. **90**, 157001 (2003).

[34] T. Maehira, T. Hotta, K. Ueda, and A. Hasegawa, Phys. Rev. Lett. **90**, 207007 (2003).

[35] T. Maehira, M. Higuchi, and A. Hasegawa, Physica B **329-333**, 574 (2003).

[36] H. Yamagami, Physica B **312-313**, 297 (2002).

[37] H. Yamagami (unpublished).
[38] H. Yamagami, Acta Phys. Pol. B **34**, 1201 (2003).
[39] Y. Tokiwa, Y. Haga, N. Metoki, Y. Ishii, and Y. Onuki, J. Phys. Soc. Jpn. **71**, 725 (2002).
[40] A. Murasik, J. Leciejewicz, S. Ligenza, and A. Zygmunt, Phys. Status Solidi A **23**, K147 (1974).
[41] A.C. Lawson, A. Williams, J.L. Smith, P.A. Seeger, J.A. Goldstone, J.A. O'Rourke, and Z. Fisk, J. Magn. Magn. Mater. **50**, 83 (1985).
[42] P. Dervenagas, D. Kaczorowski, F. Bourdarot, P. Burlet, A. Czopnik, and G.H. Lander, Physica B **269**, 368 (1999).
[43] F. Izumi and T. Ikeda, Mater. Sci. Forum **321-324**, 198 (2000).
[44] A. Hiess, F. Boudarot, S. Coad, P.J. Brown, P. Burlet, G.H. Lander, M.S.S. Brooks, D. Kaczorowski, A. Czopnik, and R. Troc, Europhys. Lett. **55**, 267 (2001).
[45] G.H. Lander, in *Handbook on the Physics and Chemistry of Rare Earths*, edited by K.A. Gschneidner, Jr., L. Eyring, G.H. Lander, and G.R. Choppin (Elsevier, Amsterdam, 1993), Vol. 17, p. 635.
[46] M. Nakamura, Y. Koike, N. Metoki, K. Kakuhira, Y. Haga, G.H. Lander, D. Aoki, and Y. Onuki, J. Phys. Chem. Solids **63**, 1193 (2002).
[47] S. Ikeda, N. Metoki, Y. Haga, K. Kaneko, T. D. Matsuda, and Y. Onuki, J. Phys. Soc. Jpn. (to be published).
[48] D. Aoki, N. Suzuki, K. Miyake, Y. Inada, R. Settai, K. Sugiyama, E. Yamamoto, Y. Haga, Y. Onuki, T. Inoue, K. Kindo, H. Sugawara, H. Sato, and H. Yamagami, J. Phys. Soc. Jpn. **70**, 538 (2001).
[49] S. Ikeda, Y. Tokiwa, T. Okubo, Y. Haga, E. Yamamoto, Y. Inada, R. Settai, and Y. Onuki, J. Nucl. Sci. Technol., Suppl. **3**, 206 (2002).
[50] Y. Tokiwa, K. Sugiyama, T. Takeuchi, M. Nakashima, R. Settai, Y. Inada, Y. Haga, E. Yamamoto, K. Kindo, H. Harima, and Y. Onuki, J. Phys. Soc. Jpn. **70**, 1731 (2001).
[51] H. Ptasiewicz-Bąk, J. Leciejewicz, and A. Zygmunt, J. Phys. F: Met. Phys. **11**, 1225 (1981).
[52] M. Kuznietz, H. Pinto, H. Ettedgui, and M. Melamud, Phys. Rev. B **40**, 7328 (1989).
[53] T. Endstra, G.J. Nieuwenhuys, and J.A. Mydosh, Phys. Rev. B **48**, 9595 (1993).
[54] An exception in this system is the antiferromagnetic basal layer in UCr_2Si_2 where structural phase transition from tetragonal to triclinic was only found, possibly due to the strong hybridization between U-5f and Cr-3d electrons (Ref. 57).
[55] S. Kambe, H. Kato, H. Sakai, R.E. Walstedt, D. Aoki, Y. Haga, and Y. Onuki, Phys. Rev. B **66**, 220403 (2002).
[56] D. Mannix, A. Stunault, N. Bernhoeft, L. Paolasini, G.H. Lander, C. Vettier, F. de Bergevin, D. Kaczorowski, and A. Czopnik, Phys. Rev. Lett. **86**, 4128 (2001).
[57] T.D. Matsuda, N. Metoki, Y. Haga, S. Ikeda, T. Okubo, K. Sugiyama, N. Nakamura, K. Kindo, K. Kaneko, A. Nakamura, E. Yamamoto, and Y. Onuki, J. Phys. Soc. Jpn. **72**, 122 (2003).